



Research article

The potential of terahertz sensing for cancer diagnosis

Zohreh Vafapour^{a,b,*}, Afsaneh Keshavarz^c, Hossain Ghahraloud^{d,e}^a Department of Bioengineering, University of Illinois at Chicago, Chicago, IL, 60607, USA^b Department of Electrical and Computer Engineering, University of Illinois at Chicago, Chicago, IL, USA^c Department of Physics, College of Science, Shiraz University, Shiraz, 71946, Fars, Iran^d Department of Chemical Engineering, Shiraz University, Shiraz, 71345, Fars, Iran^e Department of Chemical and Biomolecular Engineering, Johns Hopkins University, Baltimore, 21218, MD, USA

ARTICLE INFO

Keywords:

Biomedical engineering
Biophysics
Optics
Photonics
Terahertz sensing
Cancer detection
Terahertz pulse detecting method
Complex refractive index sensing
Finite difference time domain (FDTD) method
Semiconductor devices

ABSTRACT

The terahertz (THz) region lies between the microwave and infrared regions of the electromagnetic (EM) spectrum such that it is strongly attenuated by water and very sensitive to water content. Here, we numerically present what is to our knowledge the detecting system based on THz reflectance spectral responses data in the diagnosis of *in vivo* and *ex vivo* of some cancer's samples such as skin, breast and colon cancer tissue samples. The numerical analysis on the use of semiconductor metamaterial design/device as a complex refractive index (CRI) biosensor have been carried out. We demonstrate the application of terahertz pulse detecting (TPD) in reflection geometry for the study of normal and cancerous biological tissues. THz radiation has very low photon energy and thus it does not pose any ionization hazard for biological tissues. The sensitivity of THz radiation to polar molecules, such as water, makes TPD suitable to study the diseases in human body. By studying the THz pulse shape in the time domain, we have been able to differentiate between diseased and normal tissue for the study of basal cell carcinoma (BCC), breast and colon cancers. These results demonstrate the potential of TPD for the study of skin tissue and its related disorders, both *in vivo* and *ex vivo*. Findings of this study demonstrate the potential of TPD to depict breast and colon cancers and both *in vivo* and *ex vivo* of skin cancer and encourage further studies to determine the sensitivity and specificity of the technique.

1. Introduction

The development of terahertz (THz) technology has focused on the 0.1–10 THz frequency gap between photonics and electronics and initial demonstrations have generated tremendous interest in the fields of sensing and imaging (Hu and Nuss 1995; Vafapour et al., 2018a, b). THz technology plays an important role in different areas of human health activities (e.g., biological, drugs and explosions detection, imaging applications, etc.). THz reflection sensing/imaging is non-ionizing and has detection potential as a medical sensing technique; and its non-ionizing radiation may be safely used to detect different tissue types, such as normal cells and tumors (Pickwell and Wallace, 2006; Keshavarz et al., 2019a, b). From cancer research to DNA analysis, THz technology is improving or even making possible sensing, imaging, and detecting of different diseases such as skin cancer (Joseph et al., 2011), breast (Chen et al., 2011a), colon (Wahaia et al., 2011), oral (Sim et al., 2013), cervical (Jung et al., 2011) and other kinds of cancers. Nowadays, cancer development is preceded by visible mucosal changes in human life. Currently,

cancer diagnosis relies on the availability of qualified pathologists. Thus, the diagnosis workflow could benefit from the introduction of automated visualization techniques such as THz sensing (Vafapour et al., 2018a, b; Pickwell and Wallace, 2006; Keshavarz et al., 2019a, b; Keshavarz et al., 2019a, b; Tao et al., 2010; O'Hara et al., 2008; Ghafari et al., 2019; Emami Nejad et al., 2019; Vafapour, 2019; Chen et al., 2011b; Vafapour and Ghahraloud, 2018), detecting (Keshavarz et al., 2019a, b; Park et al., 2014; Yan et al., 2019; Sadeghzadeh Lari et al., 2020) and imaging (Zhang, 2002; Carranza et al., 2015; Zhou et al., 2018) approaches.

THz technology has been advancing rapidly because of its tremendous potential applications (Vafapour et al., 2018a, b; Pickwell and Wallace, 2006; Keshavarz et al., 2019a, b; Keshavarz et al., 2019a, b; Tonouchi, 2007; Mittleman et al., 1996; Ferguson and Zhang, 2002; Kawase et al., 2003; Wang and Mittleman, 2004; Withayachumnankul et al., 2007; Farmani et al., 2018; Vafapour et al., 2018; Chen et al., 2012; Zhu et al., 2014; Vafapour et al., 2018; Ma et al., 2019; Vafapour et al., 2018). Among them, THz cancer diagnosis is drawing much attention as THz electromagnetic (EM) waves can detect the variation of cells caused

* Corresponding author.

E-mail addresses: z.vafapour@jhu.edu, vafa@uic.edu (Z. Vafapour).

by cancer, thereby rendering a new modality of medical imaging (Fitzgerald et al., 2006; Pickwell and Wallace, 2006; Yin et al., 2007; Nakajima et al., 2007; Ji et al., 2019). First published results on cancer tissue imaging using THz pulsed radiation is in Ref. (Woodward et al., 2003), later confirmed by studies on various cancer types and organs in Ref. (Fitzgerald et al., 2006), suggest that THz imaging can be used for macroscopic visualization of tumor margins in fresh tissues. The THz cancer detection application is published by Keshavarz et al. (Keshavarz et al., 2019a, b) which demonstrated the possibility of using THz sensing technology in a water-based metamaterial (MM) for *in vivo* skin cancer detection. Emami Nejad et al. (Emami Nejad et al., 2019) proposed a supersensitive nano biosensor which demonstrated the enhancement of the capability of measurement and detection of cancer cells by THz sensing technology.

There are two major merits in cancer diagnosis: First, it covers a wider area compared to the optical microscopy measurements, and second, once the systematic analysis is established, it can provide an objective judgment which is independent of the skill of medical professionals. The tissue hydration studies were proposed as an initial medical application (Arnone et al., 1999; Mittleman et al., 1999). It has also been tested in skin, lung, pancreas, and breast cancer applications (Woodward et al., 2003; Fitzgerald et al., 2006; Joseph et al., 2011; Brun et al., 2010). The THz imaging, sensing and detecting approaches, which utilizes the EM radiation spectrum between 0.1 and 10 THz, have been investigated to assess their potential to diagnose cancers by measuring the water content change and cell deformation of malignant tumors (Globus et al., 2003; Pickwell and Wallace, 2006; Son, 2009; Sy et al., 2010; Park et al., 2011) or by sensing the nanoparticle probes targeted at cancerous tumors (Oh et al., 2009; Oh et al., 2011; Park et al., 2012; Son, 2013) and/or by analyzing the spectral responses EM THz wave (such as reflected, transmitted and absorbed spectra) from the sample (Keshavarz et al., 2019a, b; Emami Nejad et al., 2019) due to changes in the optical properties of the samples.

This article describes the use of various intelligent analysis approaches to choose relevant sensing parameters and optimize the processing of THz reflectance spectral responses data in the diagnosis of *in vivo* and *ex vivo* of basal cell carcinoma (BCC) skin cancer, and detect breast and colon cancer samples. We discuss the current state-of-the-art in terms of THz sensing/detecting systems; describe current applications, future potential, and our own approaches to harnessing this novel technology.

2. THz bio detector design investigation

The response of a THz sensor can be very fast, but it is noisy. A further reduction of noise is possible by using sensors with smaller active area. We proposed the optical sensor in micro-size which describe as a small device. The unit cell of the proposed THz bio sensor design which consists of double-layer dielectric material in cross shape, a glass substrate and a quartz layer as a dielectric spacer (or buffer layer) and an H-shaped semiconductor (Indium antimonide, InSb) antenna depicted schematically in Figure 1. The ground plane of quartz, with a dielectric layer spaced in between of the H-shaped semiconductor antenna and the substrate. The space between the semiconductor antenna and the glass substrate (the lowest layer in the structure) is filled by quartz as the dielectric spacer with thickness of 5 μm . Dimensions of the cross (in microns) are: 400 μm as the length and width in the x- and y-direction. The thickness of both cross-shape materials is 5 μm and thickness of the H-shaped semiconductor element is 4 μm . The other geometrical parameters are presented in Figure 1b. This two-layer dielectric and the semiconductor element couple to both the electric and magnetic components of incident THz EM waves and allows for maximization of the reflectance at a certain THz frequency. The dielectric ground plane is designed to be thick enough to prevent light transmission and therefore

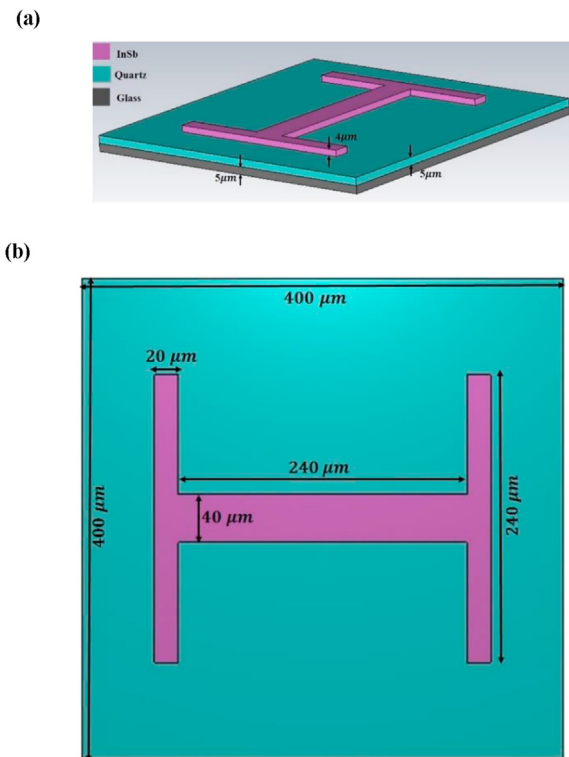


Figure 1. (a) 3D, and (b) 2D of the Schematic drawing of the THz bio detector design.

guarantees a narrow band reflection with high reflectivity to be more appropriate for fabrication process.

For numerical calculations, we used the finite time constraint (FDTD) method and used the CST Microwave Studio simulator software. For the calculations, we used a single cell, in which the lateral boundaries x and y were used as periodic boundaries, and perfectly matched layers in the z direction were considered to eliminate non-physical boundary reflections. When the wave of the plane THz EM lands vertically on the structure with polarization along the z-axis, the connection resonance must be created between the dual dielectric layer and the H-shaped semiconductor antenna. The light transmission from the whole structure is very close to zero and the resonance peak is more visible in the reflection spectrum.

3. Cancer detection potentials

Early detection of cancer greatly improves prognosis, treatment opportunities, and the chances of survival. Early detection of cancer increases treatment chances and greatly increases the chances of survival. (Alexandrov et al., 2010; Mingaleev et al., 2002; Titova et al., 2013; Bogomazova et al., 2015; Demidova et al., 2013; Saffarian and Tzeng, 2016, 2017bib_Saffarian_and_Tzeng_2017bib_Saffarian_and_Tzeng_2016). Although current screening protocols may be replaced in the future by more up-to-date and efficient technologies, developing a clear and systematic approach to early detection of cancer will lead to greater use of advanced technologies and further advances in cancer diagnosis and control. Here, we present a new and practical method using a bio-detector structure in the THz range to detect three different types of cancer (skin, breast and colon cancers) as *in vivo* and *ex vivo* detection by analyzing THz reflected waves from the cell samples suspected of cancer. First, we investigate the complex refractive index (CRI) sensing of the THz designed by calculating the THz frequency shift of the reflected spectrum and optical sensing properties of the

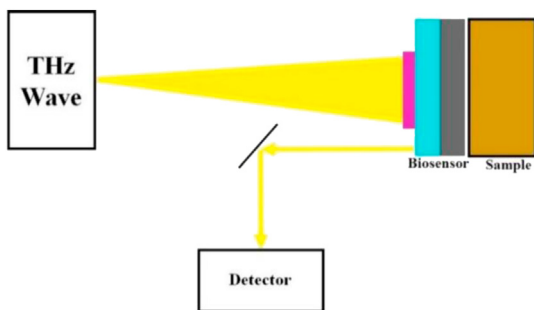


Figure 2. Schematic drawing of the THz bio detector device when the sample is investigating/testing using illumination of the THz EM wave.

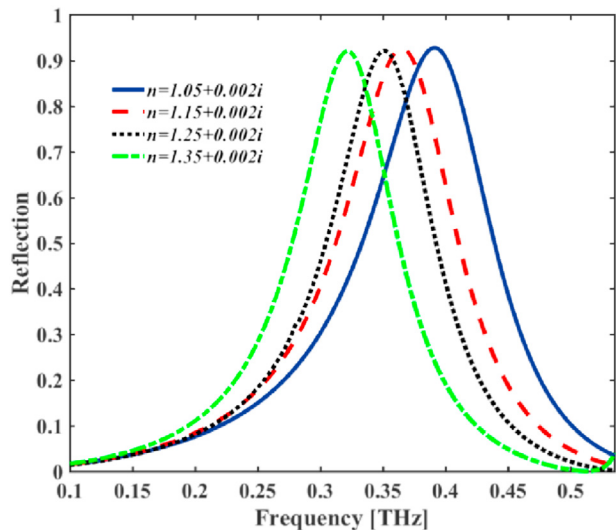


Figure 3. The simulated results of reflectance spectrum for different real parts of the CRI of the surrounding medium.

proposed design/device. Then, we analyze the reflected THz responses from different cell samples to identify normal and cancerous cells.

3.1. Complex refractive index THz sensing/detecting

To examine in more detail the performance of the THz bio detector/sensor which is shown in Figure 2, we survey the changes of the optical influential parameters and materials used in the proposed optical sensor device, such as the real and imaginary parts of the complex refractive index (CRI) of the surrounding medium/material.

The THz bio detector/sensor based on reflected EM optical responses techniques are receiving a high degree of attention because of the need to develop simple, low-cost, high-throughput detection technologies for several applications such as cancers diagnosis and virus's detection. Here, we use a THz MM design for the detection limit of resonant CRI sensors/detectors that consider all optical parameters that affect the sensing/detecting performance (Jaksic et al., 2011; Vafapour and Zakery, 2016; Vafapour and Zakery, 2015; Le et al., 2016; Vafapour 2017). This research is a common method that provides the conditions for quantifying and comparing the performance of optical biosensors based on optical resonance/detectors. Additionally, it leads to design strategies for performance improvement of CRI bio detectors/sensors for medical, chemical, and biological detection applications.

Figures 3 and 4 display the sensing performance by using the reflected spectra, where the real and imaginary parts of the CRI of surrounding medium are changed. By increasing the amount of real part of the CRI from 1.05 to 1.35, the resonant reflected THz frequency shows an apparently large red shift as shown in Figure 3, where the imaginary

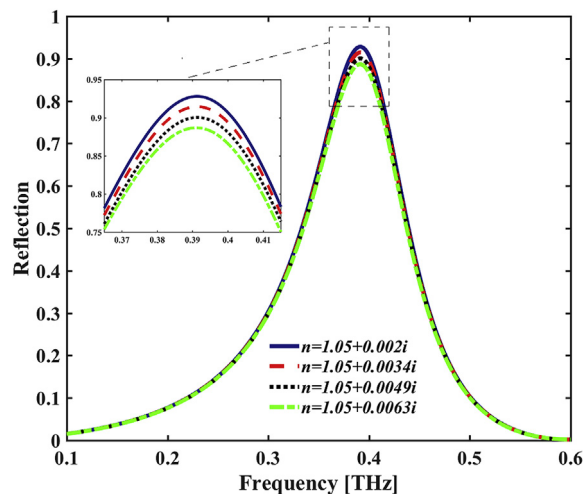


Figure 4. The simulated results of reflectance spectrum for different imaginary parts of the CRI of the surrounding medium.

parts are considered as a fixed amount of 0.002. To clearly show the shifting properties of the reflection spectrum, the frequency of the peak reflected spectra and other optical sensing properties of the design at four different values of the real parts of CRI are presented in Table 1 with the corresponding resonant wavelengths and full width at half-maximum (FWHM) values. It is shown that increasing the real part value by the step of 0.1, the resonant frequency can be red-shifted by more than 0.07 THz, i.e., the wavelength has blue-shifted by more than 167 μm. As shown in Figure 3 and Table 1. The resonance peak frequency (RP) varies, but the maximum reflected coefficients for different CRI cases are almost unchanged. So, we defined the sensitivity (S_R) as follows (Vafapour et al., 2018a, b)

$$S_R = \frac{\Delta f}{\Delta n} \tag{1}$$

where Δf defined as frequency shift of the maximum reflectance coefficient and Δn is the changes in real part of the CRI. So, we can define the figure of merit (FOM) as

$$FOM = \frac{S_R}{FWHM} \tag{2}$$

which can reach to 1.5 where the reflection coefficient is about 92.8%. Table 1 indicates that the sensitivity and FOM are $264 \frac{GHz}{RIU}$ and 1.5, respectively. Compared to the big changes in frequency shift, the reflection coefficient is nearly unchanged.

Figure 4 shows the reflectivity spectra of the proposed THz bio detector by changing the imaginary part of the CRI of the surrounding materials. Here, the reflectivity, $R(\omega)$ is defined as

$$R(\omega) = 1 - T(\omega) - A(\omega) \tag{3}$$

where $T(\omega)$ is the transmission and $A(\omega)$ is the absorption. From Figure 4, we can see that the reflectivity undergoes a small amount of decreasing when the imaginary part of the CRI increases from 0.002 to 0.063. It is noted that the reflected resonance peak is totally unchanged when the imaginary part of the CRI of sensing medium vary from 0.002 to 0.0063, but the reflection coefficient decreases by increasing the imaginary part of the CRI. Therefore, we can detect the CRI change by observing the decreasing trend of the reflectance percentage of the spectra. However, the bio sensor/detector discussed here is from a different perspective. Here, we investigate the CRI sensing/detecting reflected spectra for the first time as a THz bio sensor/detector (using the CRI and changes both parts separately). It should be noted that the resonance peak frequency has not changed, but the maximum reflected coefficients for the different

Table 1. The sensing characteristics of the THz bio detector in different amount of real part of the CRI. RP [THz]: resonance peak [THz]; Refl.: reflection; ShRP [THz]: shifts of the resonance peak; $S \left[\frac{GHz}{RIU} \right]$: sensitivity.

CRI	RP	Reflection	ShRP	S	FWHM
1.05 + 0.002i	0.3912	0.927	—	—	18
1.15 + 0.002i	0.3648	0.925	0.0264	264	176
1.25 + 0.002i	0.3510	0.922	0.0402	201	159
1.35 + 0.002i	0.3216	0.920	0.0696	232	154

Table 2. The sensing characteristics of the THz bio detector in different amount of imaginary part of the CRI.

CRI	RP	Reflection	ShRP	S	FWHM
1.05 + 0.002i	0.3912	0.927	—	—	188
1.15 + 0.0034i	0.3912	0.913	0.014	10.0	189
1.25 + 0.0049i	0.3912	0.900	0.027	9.31	190
1.35 + 0.0063i	0.3912	0.887	0.040	9.30	191

Table 3. The optical parameters of normal skin and BCC samples for the double Debye model which is presented in Eq. (5) at two different situations: *in vivo* and *ex vivo* Vafapour, 2017.

	ϵ_∞	ϵ_s	ϵ_2	τ_1 [Ps]	τ_2 [Ps]
<i>Ex vivo</i> normal skin	2.58	14.7	4.16	1.45	0.0611
<i>Ex vivo</i> BCC	2.65	17.6	4.23	1.55	0.0614
<i>In vivo</i> normal skin	3.4	25	5.0	7.0	1.0
<i>In vivo</i> BCC	4.2	40	6.2	10.0	1.0

CRI in the table have changed (see Figure 4 and Table 2). Therefore, we defined the sensitivity (S_I) as

$$S_I = \frac{\Delta R}{\Delta k} \tag{4}$$

where ΔR defined as shift of reflectivity and Δk is the changes in imaginary part of the CRI.

3.2. Skin cancer diagnosis

Excessive exposure of skin tissue to ionizing UV radiation can cause DNA damage and mutations, which leads to transformation and uncontrolled proliferation of basal cells, creating tumors known as basal cell carcinoma (BCC) (Yu et al., 2012). Early diagnosis of this type of tumor accelerates the recovery process, and treatment be easier and less costly. Since basal cells form the deepest layer of epidermis (outermost layer of skin), they are not visible, making the early diagnosis of BCC difficult. Today, many articles have examined the differences in water content and water binding status in normal and cancerous tissues (Pickwell et al., 2004a, b). Because the THz EM wave is very sensitive to polar materials, including water, and reacts clearly to polar material, we recommended using THz EM wave imaging to detect BCCs. Many researchers have modelled healthy skin and the BCC with the double Debye model (Pickwell et al., 2004a, b).

$$\epsilon(\omega) = \epsilon_\infty + \frac{\epsilon_s - \epsilon_2}{1 + i\omega\tau_1} + \frac{\epsilon_2 - \epsilon_\infty}{1 + i\omega\tau_2} \tag{5}$$

where ϵ_∞ , ϵ_s , ϵ_2 , τ_1 and τ_2 are temperature dependent of high frequency permittivity, static dielectric constant, intermediate frequency limit, slow relaxation time, and fast relaxation time, respectively. As we know, the tissues of the human body are examined in two types of *ex vivo* and *in vivo* situations. *Ex vivo* refers to experiments and measurements in which the tissue is examined in an environment outside of the living creature with minimal change of conditions. *In vivo* refers to experiments and measurements that the tissue is examined inside the living organism.

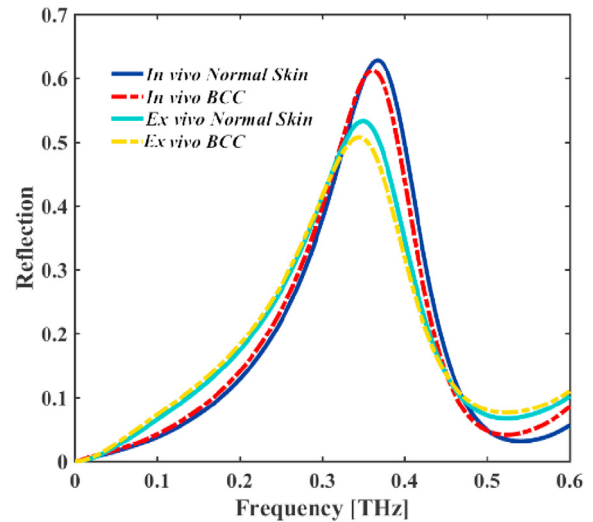


Figure 5. The reflected spectra THz EM wave of the design came from normal skin (solid-curves) and BCC (dashed-curves) cell samples into different situations: *in vivo* and *ex vivo*.

Undoubtedly, experiments in *in vivo* are realistic and provide more accurate results, but the experimental conditions are more difficult in this case. Here, we investigate to detect the normal and cancerous samples in both cases. The optical constants and parameters in the double Debye model (Equation 5) for healthy skin and BCC for *ex vivo* and *in vivo* (Pickwell et al., 2005) are presented in Table 3.

By putting the THz detector on a skin suspected of cancer, and normally shine the THz EM wave to the optical bio sensor/detector, the reflection spectrum of the sensor will be different for healthy and cancerous skin (see Figure 5). The reflection spectra of healthy skin and BCC for *ex vivo* and *in vivo* are shown in Figure 5. As shown in Figure 5,

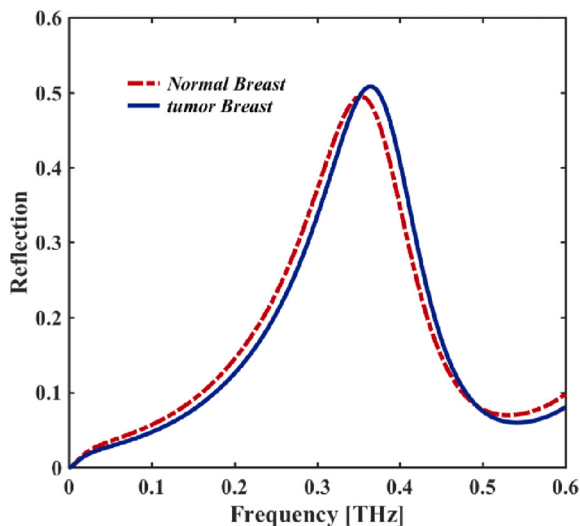


Figure 6. The reflected spectra THz EM wave of the design came from normal breast and the tumor breast cell samples.

the difference between normal and cancerous skin (BCC) for *in vivo* case is greater than *ex vivo*. The reflection spectrum of BCC sample for *ex vivo* case is about 50.76% at $\omega_1 = 0.345$ THz which is slightly red shifted in compression with normal skin tissue sample with high reflection coefficient of 53.26% at $\omega_2 = 0.35$ THz. Also, the reflection spectrum for BCC sample for *in vivo* case is approximately 61.2% at $\omega_3 = 0.361$ THz which is red shifted in compression with normal skin tissue sample with high reflection coefficient of 62.81% at $\omega_4 = 0.368$ THz. Therefore, it can be concluded that examining skin suspected of having cancer gives clearer results for *in vivo* than the *ex vivo* method. .

3.3. Breast cancer diagnosis

Breast cancer is the most common type of cancer for women around the world. Each year, the breast cancer has a high rate of female mortality (Bray et al., 2018). According to the studies, if diagnosis of breast cancer is faster, treatment is easier and less costly (Tayel et al., 2018). One of the most common imaging techniques for diagnosing breast cancer is x-ray mammography. However, this method is harmful to body tissues due to the use of ionizing X-rays and should not be used too many times (Oh et al., 2009). In addition, this method requires the compression of the breast, which causes the person to suffer a lot (Sugitani et al., 2014). Other methods, including magnetic resonance imaging (MRI) and ultrasound are also used to diagnose breast cancer; but they are so expensive (Nilavalan et al., 2007). One of the newest methods for detecting breast cancer is ultra-wideband (UWB) method (Wang et al., 2014). The design of UWB transmit focusing is more complex and UWB focusing yields higher absorbed power near the surface of the breast (Elkayal et al., 2015).

In this work, we propose a method for detecting a healthy breast tissue in compression with cancerous breast tissue by using a THz bio detector. In this method, we put the THz MM designed as the bio detector too close to the breast tissue; and by observing the reflectance spectrum of the biosensor, we can identify the tissue's healthy or cancerous nature (see Figure 6). The reflection spectrum of tumor breast sample is about 49.45% at $\omega_1 = 0.352$ THz which is red shifted in

compression with normal breast tissue sample with high reflection coefficient of 50.78% at $\omega_2 = 0.365$ THz. In this section, we took an idea from the method presented in (Cassar et al., 2018) to simulate normal breast tissue and breast cancer tissue. . In (Fitzgerald et al., 2014), Fitzgerald et al. used the Debye model (presented in Eq.5) for healthy and cancerous breast tissues. Constants for this modelling are given in Table 4 and plotted in Figure 7.

3.4. Colon cancer diagnosis

Colon cancer is the third most common cancer in the world between men and women. Because the disease progresses slowly, early diagnosis of colon cancer has a tremendous effect on the treatment of the disease. So, early detection is very necessary. Optical methods are used to detect colon cancer using different frequencies. For example, Shmuel Argov et al., in 2002 (Argov et al., 2002) have proposed a method for the diagnosis of colon cancer using infrared radiation. Recently, THz imaging has been suggested for colon cancer imaging via an endoscope, and work is progressing in creating and testing endoscopic THz systems (Wang et al., 2014; Ji et al., 2009; Chen et al., 2011a). In other words, THz radiation is more useful than other frequencies for diagnosing colon cancer for a number of reasons, including non-ionization and high resolution. (Wallace et al., 2008). Currently, the only previous published work on THz imaging of colon cancer is that of Reid et al. (2011), whose data is reanalyzed in the current research using our method by analyzing the reflected spectral responses. Their results are not listed here but full details can be found in their publication (Reid et al., 2011). Using their parameters, they reported the absorption coefficient and RI of the healthy and abnormal tissues (cancerous tissues). Using the formulas $\epsilon = \epsilon_1 + i\epsilon_2$ for the permittivity of colon tissue, we can calculate the shift in reflection and absorption coefficient and RI relate to the real and imaginary part of the permittivity. The real and imaginary parts of permittivity are calculated as $\epsilon_1 = n^2 - \kappa^2$ and $\epsilon_2 = 2n\kappa$, in which $\kappa = \frac{\alpha c}{\omega}$; where κ , n , c , α and ω respectively are the imaginary part of the RI, real part of the RI, speed of light in the vacuum, absorption coefficient, and $\omega = 2\pi f$ in which f is the frequency of the light shining.

We introduce a method to distinguish between healthy and cancerous tissues samples. In this method, the difference of interaction between the healthy and cancerous colon tissues with THz radiation is due to the cancerous tissue contains more water than healthy tissue, and the polar molecules of the water absorb THz waves more, so, the reflection of the cancerous colon tissue is less than normal colon tissue sample (see Figure 8).

Here, we insert the proposed THz MM in front of the colon tissue samples and shine the normal incidence of THz EM wave on it. By analyzing the reflectance spectrum of the optical bio detector device, we can identify the tissue's healthy or cancerous nature (see Figure 8). As it is clearly shown in Figure 8, the reflection spectrum of the bio detector is different for healthy and cancerous tissue samples. The reflection spectrum of cancerous colon tissue is slightly red shifted in compression with normal colon tissue sample and the maximum peak reflection coefficient for the normal tissue sample is more than 50% (it is about 52.4% at $\omega_2 = 0.36$ THz), but for the cancerous tissue sample less than 50% (it is approximately 48.7 % at $\omega_1 = 0.35$ THz). The reflected spectrum of the cancerous colon tissue is decreased because the more than 50% of the THz wave is absorbed by water in the cancerous colon tissue.

Table 4. The optical parameters of normal breast and tumor breast samples for the double Debye model in which is presented in Eq. (5) (Fitzgerald et al., 2014).

	ϵ_∞	ϵ_s	ϵ_2	τ_1 [Ps]	τ_2 [Ps]
Normal breast	2.1	76.5	3.9	10.3	0.07
Tumor breast	2.5	77.9	4.3	9.1	0.08

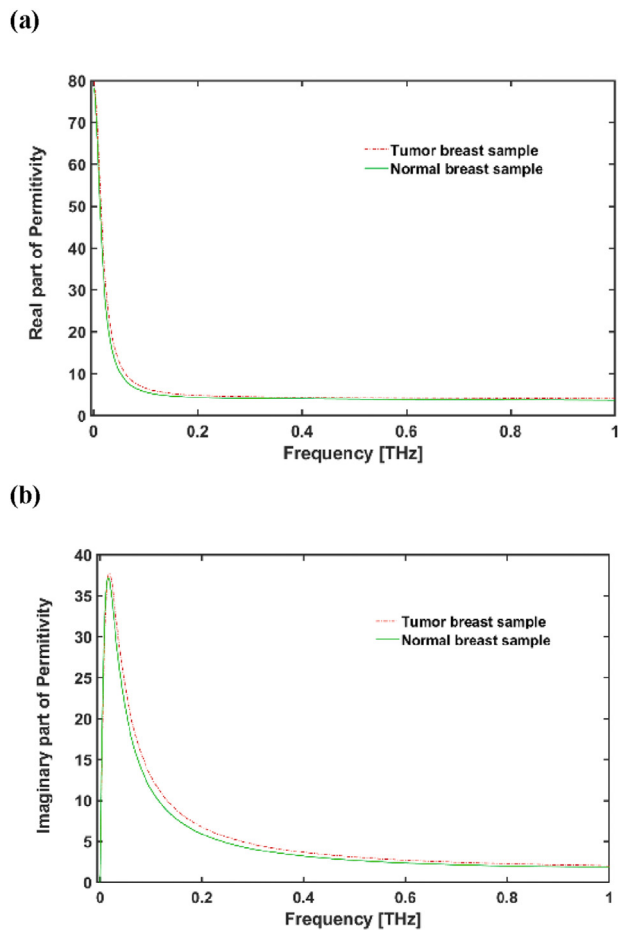


Figure 7. (a) The imaginary, and (b) real parts of the permittivity for healthy and cancerous breast tissue samples.

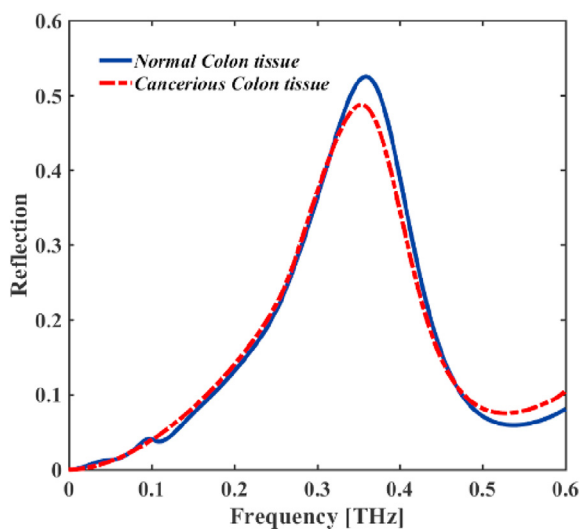


Figure 8. The reflected spectra THz EM wave of the design came from normal colonic tissue and the cancerous colonic tissues.

4. Future directions and conclusions

Terahertz imaging, sensing, and detecting are still in the early stages of development. THz Pulsed Detecting (TPD) is a new opto-medical detecting modality for the detection of epithelial cancers. The presence of cancer often causes increased blood supply to affected tissues and a

local increase in tissue water content may be observed. Furthermore, the structural changes that occur in affected tissues which causes changing the complex refractive index of the tissues have been used to contribute to THz detecting technology. By comparing/analyzing the reflected THz spectral responses from the tissue, the circumstances of the tissue sample can be detectable. This acts as so new and updated mechanism for THz detecting of cancer. Nowadays, this technique is improving to apply to the study of *in vivo* and *ex vivo* basal cell carcinoma (BCC) of skin cancer. This paper introduces THz technology and provides a recipe in the THz sensing and detecting techniques. Using time-domain analysis the contrast between diseased and normal tissue has been shown to be statistically significant, and regions of decreased THz reflection (increased THz absorption). Using the complex refractive index and reflection coefficient spectra of healthy and diseased cancerous tissue, we could detect three kinds of cancers (skin, breast and colon cancers). Comparisons of the differences between the spectra of different tissue types were made. Simulations were carried out to show the impulse responses from performing THz pulsed reflection to detect the kind of the tissue samples. A large difference was seen, as PREDICTED, between the impulse response of healthy and those of cancerous tissues. A difference in peak height and frequency shift of the reflected impulse responses between cancerous and healthy tissue is shown. Such difference encourages the development of opto-medical devices based on THz technology. This new technology will improve and enhance detecting techniques available to clinicians for improvement of cancer treatment and healthcare in general.

Declarations

Author contribution statement

Zohreh Vafapour: Conceived and designed the experiments; Analyzed and interpreted the data; Wrote the paper.

Afsaneh Keshavarz: Performed the experiments; Analyzed and interpreted the data.

Hossain Ghahraloud: Analyzed and interpreted the data; Wrote the paper.

Funding statement

This research did not receive any specific grant from funding agencies in the public, commercial, or not-for-profit sectors.

Data availability statement

Data included in article/referenced in article.

Competing interest statement

The authors declare no conflict of interest.

Additional information

No additional information is available for this paper.

Acknowledgements

The authors would like to express their special thanks to Dr. Reza Behrouzi from Department of Cell Biology, Harvard Medical School, professor Mitra Dutta from Physics, and Electrical and Computer Engineering departments of the University of Illinois at Chicago and Professor Michael A. Strosio from Departments of Bioengineering, Physics, and Electrical and Computer Engineering departments of the University of Illinois at Chicago for their useful discussions.

References

- Alexandrov, B.S., Gelev, V., Bishop, A.R., Usheva, A., Rasmussen, K.Ø., 2010. DNA breathing dynamics in the presence of a terahertz field. *Phys. Lett.* 374 (10), 1214–1217.
- Argov, S., Rameshm, J., Salman, A., Sinelnikov, I., Goldstein, J., Guterman, H., Mordechai, S., 2002. Diagnostic potential of Fourier-transform infrared microspectroscopy and advanced computational methods in colon cancer patients. *J. Biomed. Optic.* 7 (2), 248–255.
- Arnone, D.D., Ciesla, C.M., Corchia, A., Egusa, S., Pepper, M., Chamberlain, J.M., Bezant, C., Linfield, E.H., Clothier, R., Khammo, N., 1999. Applications of terahertz (THz) technology to medical imaging. *Proc. SPIE* 3828, 209–219.
- Bogomazova, A.N., Vassina, E.M., Goryachkovskaya, T.N., Popik, V.M., Sokolov, A.S., Kolchanov, N.A., Lagarkova, M.A., Kiselev, S.L., Peltek, S.E., 2015. No DNA damage response and negligible genome-wide transcriptional changes in human embryonic stem cells exposed to terahertz radiation. *Sci. Rep.* 5, 7749.
- Bray, F., Ferlay, J., Soerjomataram, I., Siegel, R.L., Torre, L.A., Jemal, A., 2018. Global cancer statistics 2018: GLOBOCAN estimates of incidence and mortality worldwide for 36 cancers in 185 countries. *CA A Cancer J. Clin.* 68 (6), 394–424.
- Brun, M.A., Formanek, F., Yasuda, A., Sekine, M., Ando, N., Eishii, Y., 2010. Terahertz imaging applied to cancer diagnosis. *Phys. Med. Biol.* 55, 4615–4623.
- Carranza, I.E., Grant, J., Gough, J., Cumming, D.R., 2015. Metamaterial-based terahertz imaging. *IEEE Trans. on THz Sci. and Tech.* 5 (6), 892–901.
- Cassar, Q., Al-ibadi, A., Mavarani, L., Hillger, P., Grzyb, J., Macgrogan, G., Zimmer, T., Pfeiffer, U.R., Guillet, J., Mounaix, P., 2018. Pilot study of freshly excised breast tissue response in the 300–600 GHz range. *Biomed. Optic Express* 9 (7), 2930.
- Chen, H., Lee, W.-J., Huang, H.-Y., Chiu, C.-M., Tsai, Y.-F., Tseng, T.-F., Lu, J.-T., Lai, W.-L., Sun, C.-K., 2011a. Performance of THz fiber-scanning near-field microscopy to diagnose breast tumors. *Optic Express* 19, 19523–19531.
- Chen, H.Z., Lu, J.Y., You, B., 2011b. Terahertz endoscope based on anti-resonant reflecting hollow core waveguides. In *Proceedings of the optical society of America conference on lasers and electro-optics (CLEO)* 1–2, May 2011.
- Chen, T., Li, S., Sun, H., 2012. Metamaterials application in sensing. *Sensors* 12 (3), 2742–2765.
- Demidova, E.V., Goryachkovskaya, T.N., Malup, T.K., Bannikova, S.V., Semenov, A.I., Vinokurov, N.A., Kolchanov, N.A., Popik, V.M., Peltek, S.E., 2013. Studying the non-thermal effects of terahertz radiation on *E. coli*/pKatG-GFP biosensor cells. *Bioelectromagnetics* 34 (1), 15–21.
- Elkayal, H.A., Ismail, N.E., Lotfy, M., 2015. Microwaves for breast cancer treatments. *Alexandria Eng. J.* 54, 1105–1113.
- Emami Nejad, H., Mir, A., Farmani, A., 2019. Supersensitive and tunable nano-biosensor for cancer detection. *IEEE Sensor. J.*
- Farmani, A., Mir, A., Bazgir, M., Zarrabi, F.B., 2018. Highly sensitive nano-scale plasmonic biosensor utilizing Fano resonance metasurface in THz range: numerical study. *Phys. E Low-dimens. Syst. Nanostruct.* 104, 233–240.
- Ferguson, B., Zhang, X.C., 2002. Materials for terahertz science and technology. *Nat. Mater.* 1, 26–33.
- Fitzgerald, A.J., Wallace, V.P., Jimenez-Linan, M., Bobrow, L., Pye, R.J., Purushotham, A.D., Arnone, D.D., 2006. Terahertz pulsed imaging of human breast tumors. *Radiology* 239, 533–540.
- Fitzgerald, A.J., Pickwell-MacPherson, E., Wallace, V.P., 2014. Use of finite difference time domain simulations and Debye theory for modelling the terahertz reflection response of normal and tumour breast tissue. *PLoS One* 9 (7), 99291.
- Ghafari, S., Forouzeshfard, M.R., Vafapour, Z., 2019. Thermo optical switching and sensing applications of an infrared metamaterial. *IEEE Sensor. J.* 20 (6), 3235–3241.
- Globus, T.R., Woolard, D.L., Khromova, T., Crowe, T.W., Bykhovskaia, M., Gelmont, B.L., Hesler, J., Samuels, A.C., 2003. THz-spectroscopy of biological molecules. *J. Biol. Phys.* 29 (2/3), 89–100.
- Hu, B.B., Nuss, M.C., 1995. Imaging with terahertz waves. *Opt. Lett.* 20 (16), 1716–1718.
- Jakšić, Z., Vuković, S., Matović, J., Tanasković, D., 2011. Negative refractive index metasurfaces for enhanced biosensing. *Materials* 4 (1), 1–36.
- Ji, Y.B., Lee, E.S., Kim, S., Son, J., Jeon, T., 2009. A miniaturized fiber-coupled terahertz endoscope system. *Optic Express* 17 (19), 17082–17087.
- Ji, Y.B., Kim, J.M., Lee, Y.H., Choi, Y., Kim, D.H., Huh, Y.M., Oh, S.J., Koh, Y.W., Suh, J.S., 2019. Investigation of keratinizing Squamous cell carcinoma of the Tongue using terahertz reflection imaging. *Journal of Infrared, Millimeter, and Terahertz Waves* 40 (2), 247–256.
- Joseph, C.S., Yaroslavsky, A.N., Neel, V.A., Goyette, T.M., Giles, R.H., 2011. Continuous wave terahertz transmission imaging of Nonmelanoma skin cancers. *Lasers in Surgery and Medicine* 43, 457–462.
- Jung, E.A., Lim, M.H., Moon, K.W., Do, Y.W., Lee, S.S., Han, H.W., Choi, H.J., Cho, K.S., Kim, K.R., 2011. Terahertz pulse imaging of micro-metastatic Lymph Nodes in early-stage cervical cancer patients. *J. Opt. Soc Korea* 15 (2), 155–160.
- Kawase, K., Ogawa, Y., Watanabe, Y., Inoue, H., 2003. Non-destructive terahertz imaging of illicit drugs using spectral fingerprints. *Opt. Express* 11 (20), 2549–2554.
- Keshavarz, A., Vafapour, Z., 2019a. Water-based terahertz metamaterial for skin cancer detection application. *IEEE Sensors Journal* 19 (4), 1519–1524.
- Keshavarz, A., Vafapour, Z., 2019b. Sensing Avian Influenza viruses using terahertz metamaterial reflector. *IEEE Sensor Journal* 19 (13), 5161–5166.
- Le, K.Q., Ngo, Q.M., Nguyen, T.K., 2016. Nanostructured metal-insulator-metal metamaterials for refractive index biosensing applications: design, fabrication, and characterization. *IEEE Journal of Selected Topics in Quantum Electronics* 23 (2), 388–393.
- Ma, C.W., Ma, W., Tan, Y., Tang, Y., 2019. A terahertz metamaterial analog of electromagnetically induced transparency and its application in loss detection. In: *9th International Symposium on Advanced Optical Manufacturing and Testing Technologies: Micro-and Nano-Optics, Catenary Optics, and Subwavelength Electromagnetics* 10840, 108400R. International Society for Optics and Photonics.
- Mingaleev, S.F., Gaididei, Y.B., Christiansen, P.L., Kivshar, Y.S., 2002. Nonlinearity-induced conformational instability and dynamics of biopolymers. *EPL (Europhysics Letters)* 59 (3), 403.
- Mittleman, D.M., Jacobsen, R.H., Nuss, M.C., 1996. T-ray imaging. *IEEE J. Sel. Top. Quantum Electron.* 2, 679–692.
- Mittleman, D.M., Gupta, M., Neelamani, R., Baraniuk, R.G., Rudd, J.V., Koch, M., 1999. Recent advances in terahertz imaging. *Applied Physics B* 68, 1085–1094.
- Nakajima, S., Hoshina, H., Yamashita, M., Otani, C., Miyoshi, N., 2007. Terahertz imaging diagnostics of cancer tissues with a chemometrics technique. *Appl. Phys. Lett.* 90, 041102/1–3.
- Nilavalan, R., Craddock, I.J., Preece, A., Leendertz, J., Benjamin, R., 2007. Wideband microstrip patch antenna design for breast cancer tumour detection. *IET Microw. Antennas Propag* 1 (2), 277–281.
- Oh, S.J., Kang, J.Y., Maeng, I.H., Suh, J.S., Huh, Y.M., Haam, S.J., Son, J.H., 2009. Nanoparticle-enabled terahertz imaging for cancer diagnosis. *Opt. Express* 17 (5), 3469–3475.
- Oh, S.J., Choi, J.H., Maeng, I.H., Park, J.Y., Lee, K.G., Huh, Y.M., Suh, J.S., Haam, S.J., Son, J.H., 2011. Molecular imaging with terahertz waves. *Opt. Express* 19 (5), 4009–4016.
- O'Hara, J.F., Singh, R., Brener, I., Smirnova, E., Han, J.F., Taylor, A.J., Zhang, W., 2008. Thin-film sensing with planar terahertz metamaterials: sensitivity and limitations. *Opt. Express* 16 (3), 1786–1795.
- Park, J.Y., Choi, H.J., Cho, K.S., Kim, K.R., Son, J.H., 2011. Terahertz spectroscopic imaging of a rabbit VX2 hepatoma model. *J. Appl. Phys.* 109 (6), 064704.
- Park, J.Y., Choi, H.J., Nam, G.E., Cho, K.S., Son, J.H., 2012. In vivo dual-modality terahertz/magnetic resonance imaging using superparamagnetic iron oxide nanoparticles as a dual contrast agent. *IEEE Trans. THz Sci. Technol.* 2 (1), 93–98.
- Park, S.J., Hong, J.T., Choi, S.J., Kim, H.S., Park, W.K., Han, S.T., Park, J.Y., Lee, S., Kim, D.S., Ahn, Y.H., 2014. Detection of microorganisms using terahertz metamaterials. *Scientific Reports* 4, 4988.
- Pickwell, E., Wallace, V.P., 2006. Biomedical applications of terahertz technology. *J. of Physics D: Applied Physics* 39 (17), R301–310.
- Pickwell, E., Cole, B.E., Fitzgerald, A.J., Wallace, V.P., Pepper, M., 2004a. Simulation of terahertz pulse propagation in biological systems. *Appl. Phys. Lett.* 84 (12), 2190.
- Pickwell, E., BCoole, E., Fitzgerald, A.J., Pepper, M., Wallace, V.P., 2004b. In vivo study of human skin using pulsed terahertz radiation. *Phys. Med. Biol.* 49, 1595–1607.
- Pickwell, E., Fitzgerald, A.J., Cole, B.E., Taday, P.F., Pye, R.J., Ha, T., Pepper, M., 2005. Simulating the response of terahertz radiation to basal cell carcinoma using ex vivo spectroscopy measurements. *J. of Biomedical Optics* 10 (6), 064021.
- Reid, C.B., Fitzgerald, A., Reese, G., Goldin, R., Tekkis, P., O'Kelly, P.S., Pickwell-MacPherson, E., Gibson, A.P., Wallace, V.P., 2011. Terahertz pulsed imaging of freshly excised human colonic tissues. *Physics in Medicine and Biology* 56, 4333–4353.
- Sadeghzadeh Lari, E., Vafapour, Z., Ghahraloud, H., 2020. Optically tunable triple-band perfect absorber for nonlinear optical liquids sensing. *IEEE Sensors Journal*.
- Saffarian, M., Tzeng, J., 2016. The Effect of MazF, Escherichia coli Ribonuclease, on Gastric Adenocarcinoma (AGS cells).
- Saffarian, M., Tzeng, J., 2017. Exclusive Delivery of mazF in Cancer Cells by Listeria Monocytogenes.
- Sim, Y.C., Park, J.Y., Ahn, K.M., Park, C., Son, J.H., 2013. Terahertz imaging of excised oral cancer at frozen temperature. *Biomedical Optics Express* 4 (8), 1413–1421.
- Son, J.H., 2009. Terahertz electromagnetic interactions with biological matter and their applications. *J. Appl. Phys.* 105 (10), 102033.
- Son, J.H., 2013. Principle and applications of terahertz molecular imaging. *Nanotechnology* 24 (21), 214001.
- Sugitani, T., Kubota, Kuroki, S., Sogo, K., Arihiro, K., Okada, M., Kadoya, T., Hide, M., Oda, M., Kikkawa, T., 2014. Complex permittivities of breast tumor tissues obtained from cancer surgeries. *Appl. Phys. Lett.* 104, 253702.
- Sy, S., Huang, S., Wang, Y.X., Yu, J., Ahuja, A.T., Zhang, Y.T., Pickwell-MacPherson, E., 2010. Terahertz spectroscopy of liver cirrhosis: investigating the origin of contrast. *Phys. Med. Biol.* 55 (24), 7587–7596.
- Tao, H., Strikwerda, A.C., Liu, M., Mondia, J.P., Ekmekci, E., Fan, K., Kaplan, D.L., Padilla, W.J., Zhang, X., Averitt, R.D., Omenetto, F.G., 2010. Performance enhancement of terahertz metamaterials on ultrathin substrates for sensing applications. *Applied Physics Letters* 97 (26), 261909.
- Tayel, M.B., Abouelnaga, T.G., Desouky, A.F., 2018. UWB High Gain Antenna Array for SAR Based Breast Cancer Detection System. *the 5th International Conference on Electrical and Electronics Engineering*.
- Titova, L.V., Ayesheshim, A.K., Golubov, A., Rodriguez-Juarez, R., Woycicki, R., Hegmann, F.A., Kovalchuk, O., 2013. Intense THz pulses down-regulate genes associated with skin cancer and psoriasis: a new therapeutic avenue. *Scientific reports* 3, 2363.
- Tonouchi, M., 2007. Cutting-edge terahertz technology. *Nature Photonics* 1, 97–105.
- Vafapour, Z., 2017. Near infrared biosensor based on classical electromagnetically induced reflectance (CI-EIR) in a planar complementary metamaterial. *Optics Communications* 387, 1–11.
- Vafapour, Z., 2018. Slowing down light using terahertz semiconductor metamaterial for dual-band thermally tunable modulator applications. *Appl. Opt.* 57 (4), 722–729.

- Vafapour, Z., 2018a. Large group delay in a microwave metamaterial analog of electromagnetically induced reflectance. *J. Opt. Soc. Am. A* 35 (3), 417–422.
- Vafapour, Z., 2018b. Slow light modulator using semiconductor metamaterial. *Integrated Optics: Devices, Materials, and Technologies XXII* 10535, 105352A.
- Vafapour, Z., 2019. Polarization-independent perfect optical metamaterial absorber as a glucose sensor in Food Industry applications. *IEEE Transactions on NanoBioscience* 18 (4), 622–627.
- Vafapour, Z., Ghahraloud, H., 2018. Semiconductor-based far-infrared biosensor by optical control of light propagation using THz metamaterial. *J. Opt. Soc. Am. B* 35 (5), 1192–1199.
- Vafapour, Z., Zakery, A., 2016. New approach of plasmonically induced reflectance in a planar metamaterial for plasmonic sensing applications. *Plasmonics* 11 (2), 609–618.
- Vafapour, Z., Zakery, A., 2015. New regime of plasmonically induced transparency. *Plasmonics* 10 (6), 1809–1815.
- Wahaia, F., Valusis, G., Bernardo, L.M., Almeida, A., Moreira, J.A., Lopes, P.C., Macutkevicius, J., Kasalynas, I., Seliuta, D., Adomavicius, R., Henrique, R., Lopes, M., 2011. Detection of colon cancer by terahertz techniques. *J. of Molecular Structure* 1006, 77–82.
- Wallace, V.P., Pickwell-MacPherson, E., Zeitler, J.A., Reid, C., 2008. Three-dimensional imaging of optically opaque materials using nonionizing terahertz radiation. *Opt. Soc. Am. A* 25 (12), 3120–3133.
- Wang, K., Mittleman, D.M., 2004. Metal wires for terahertz wave guiding. *Nature* 432, 376–379.
- Wang, Z., Lim, E.G., Tang, Y., Leach, M., 2014. Medical applications of microwave imaging. *The Scientific World Journal* 147016.
- Withayachumnankul, W., Png, G.M., Yin, X., Atakaramians, S., Jones, I., Lin, H., Ung, B.S.Y., Balakrishnan, J., Ng, B.W.H., Ferguson, B., Mickan, S.P., Fischer, B.M., Abbott, D., 2007. T-Ray sensing and imaging. *Proc. IEEE* 95, 1528–1558.
- Woodward, R.M., Wallace, V.P., Pye, R.J., Cole, B.E., Arnone, D., Linfield, E.H., Pepper, M., 2003. Terahertz pulse imaging of ex vivo basal cell carcinoma. *J. Invest. Dermatol.* 120, 72–78.
- Yan, X., Yang, M., Zhang, Z., Liang, L., Wei, D., Wang, M., Zhang, M., Wang, T., Liu, L., Xie, J., Yao, J., 2019. The terahertz electromagnetically induced transparency-like metamaterials for sensitive biosensors in the detection of cancer cells. *Biosensors and Bioelectronics* 126, 485–492.
- Yin, X., Ng, B.W.H., Abbott, D., Ferguson, B., Hadjilucas, S., 2007. Application of autoregressive models of wavelet sub-bands for classifying terahertz pulse measurements. *J. Biol. Syst.* 15, 551–571.
- Yu, C., Fan, S., Sun, Y., Pickwell-MacPherson, E., 2012. The potential of terahertz imaging for cancer diagnosis: a review of investigations to date. *Quant Imaging Med Surg* 2 (1), 33–45.
- Zhang, X.C., 2002. Terahertz wave imaging: horizons and hurdles. *Physics in Medicine & Biology* 47 (21), 3667.
- Zhou, Z., Zhou, T., Zhang, S., Shi, Z., Chen, Y., Wan, W., Li, X., Chen, X., Gilbert Corder, S.N., Fu, Z., Chen, L., 2018. Multicolor T-ray imaging using multispectral metamaterials. *Advanced Science* 5 (7), 1700982.
- Zhu, J., Ma, Z., Sun, W., Ding, F., He, Q., Zhou, L., Ma, Y., 2014. Ultra-broadband terahertz metamaterial absorber. *Appl. Phys. Lett.* 105 (2), 021102.